ACS APPLIED MATERIALS & INTERFACES

Research Article

Cite This: ACS Appl. Mater. Interfaces 2019, 11, 20200−20204

www.acsami.org

Separation in the Roles of Carrier Transport and Light Emission in Light-Emitting Organic Transistors with a Bilayer Configuration

Hui Shang,[†,§] Hidekazu Shimotani,[*,†] Thangavel Kanagasekaran,[‡,⊥] and Katsumi Tanigaki[*,‡]

[†]Department of Physics, Tohoku University, 6-3, Aramaki Aza-Aoba, Aoba-ku, Sendai 980-8578, Japan

[‡]Advanced Institute for Materials Research (AIMR), Tohoku University, 2-2-1 Katahira, Aoba-ku, Sendai 980-8577, Japan

Supporting Information

ABSTRACT: To develop high-performance organic light-emitting organic field-effect transistors (LE-OFETs), a fundamental problem in organic semiconductors is to compromise light luminescent efficiency for high carrier mobility and vice versa. Therefore, LE-OFETs can avoid this problem by separating the light-emission and carrier-transport functions. Here, a bilayer LE-OFET composed of a tetracene crystal as a carrier transporter (bottom crystal) and a 4-(dicyanomethylene)-2-methyl-6-(*p*-dimethylaminostyryl)-4*H*-pyran (DCM1)-doped tetracene crystal as a light emitter (top crystal) was fabricated. Red light-emission color, which is distinct from the green emission color of tetracene, was detected in the top crystal. Light emission from the top layer was prohibited when an insulating thin film was inserted between the two crystals. These observations indicate that excitons are formed in the bottom crystal and transferred to the top crystal, emitting reddish light. Bilayer LE-OFETs have the advantage of providing both high current density and a bright emission for high-performance light-emitting FETs.

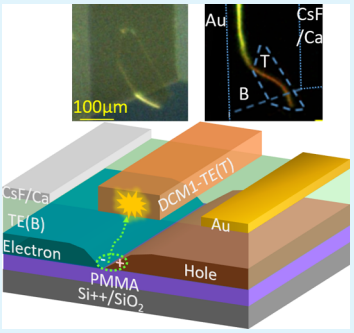

KEYWORDS: *organic light-emitting transistor, singlet fission, delayed fluorescence, long exciton diffusion length, energy transfer, bilayer device structure, separated functions*

INTRODUCTION

Light-emitting organic field-effect transistors (LE-OFETs) are nothing but ambipolar OFETs employing a fluorescent semiconductor, where a p−n junction is electrostatically formed (Figure 1a). There have been various investigations into LE-OFETs mainly from two viewpoints. First, they are novel light-emitting devices that have on−off switching, tunable emission intensity, and tunable emission position.[1] Second, they are expected to be a key component of current-driven organic semiconductor lasers in the future.[2−11] One of the most serious difficulties in the development of high-performance LE-OFETs is synthesizing suitable organic semiconductors with high carrier mobilities and high luminescent efficiency. Unfortunately, organic semiconductors generally do not demonstrate excellency in both carrier mobility and luminescent efficiency.[12−16] Therefore, it is necessary to develop a new device structure to achieve both high carrier mobility and high luminescent efficiency. Here, we provide a new device structure that divides the carrier-transport light-emission function into two distinct functions by fabricating an LE-OFET with an active layer that consists of two separate layers. Figure 1b shows a schematic diagram of the bilayer LE-OFET proposed in this study. The bottom crystal acts as a carrier transporting layer with high carrier mobility, and the top crystal performs as a light emitter with a high luminescent efficiency. Excitons are formed in the bottom layer, through the recombination of injected electrons and holes, and diffused to the top crystal.

For efficient exciton transfer from the bottom layer to the top, the exciton diffusion length (L_{ex}) in the bottom crystal must be longer than the thickness of the bottom crystal (several hundred nanometers). However, the L_{ex} of singlet excitons is reported to be several nanometers.[17−19] On the other hand, the L_{ex} of triplet excitons is much longer than those of singlet excitons, but their optical transitions are forbidden.[20−22] However, a combination of singlet fission (an excited singlet state molecule shares its excitation energy with another molecule in the ground state, and they are converted into two excited triplet state molecules) and triplet fusion (its inverse process) enables light emission after long-range exciton diffusion, as illustrated in Figure 1c. Such a process is called delayed fluorescence,[23,24] and it is observed in several organic single crystals such as rubrene,[20] tetracene,[21] and anthracene.[25] For example, Najafov et al. evaluated the L_{ex} to be in the range of 3−8 μm for a rubrene single crystal.[20] For this study, a tetracene single crystal was chosen for the transport layer, considering the high carrier mobility.[26] It was estimated that more than 99% of singlets in a tetracene thin film are converted into triplet pairs.[27]

A dye-incorporated tetracene single crystal was employed as the emission layer. This is known to be a good method for achieving both energy-band-gap matching, which is required for efficient exciton transfers, and high luminescent effi-

Received: February 12, 2019
Accepted: May 16, 2019
Published: May 24, 2019

DOI: 10.1021/acsami.9b02298
ACS Appl. Mater. Interfaces 2019, 11, 20200−20204

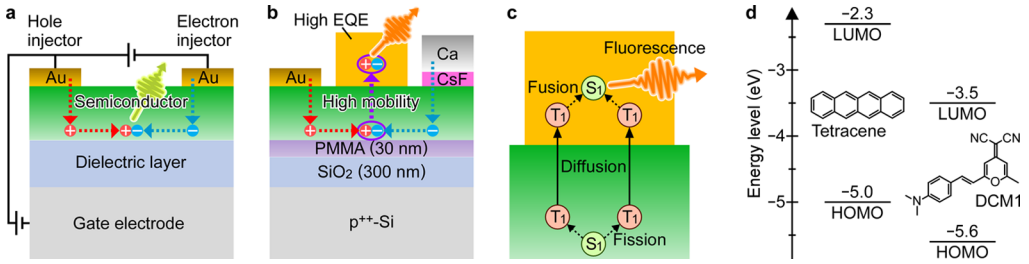

Figure 1. Proposed device structure and its components in active layer. (a) Schematic side-view diagram of an LE-OFET. (b) Schematic diagram of a bilayer LE-OFET. The bottom green layer stands for carrier transporter, and the top yellow layer acts as a light emitter. Excitons generated at the bottom layer diffuse to the top layer and emit light. (c) Schematic diagram of delayed fluorescence. A generated singlet (green circle) will share energy with its adjacent molecule forming two triplets (red circles), which have long lifetimes and diffusion lengths. Finally, two triplets can form one singlet after long-distance diffusion. (d) Molecular structures and calculated frontier orbitals of the host tetracene and guest DCM1.

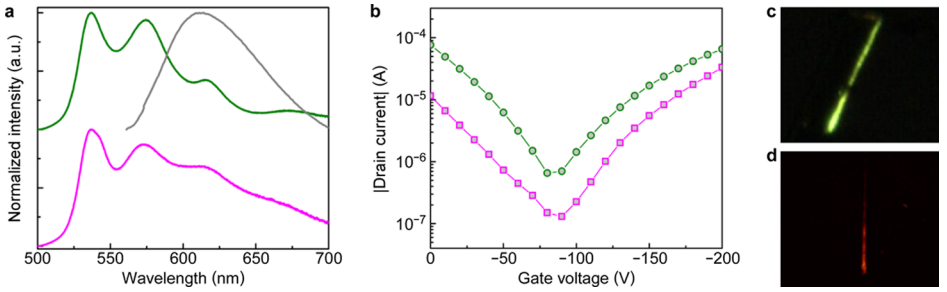

Figure 2. Optoelectronic properties of the DCM1-doped tetracene crystal. (a) Fluorescent spectra of tetracene crystals (green curve), dichloromethane solution of DCM1 (gray curve) and DCM1-doped tetracene crystals (pink curve). (b) Transfer curves of a pure tetracene crystal FET (green) and a DCM1-doped tetracene crystal FET (pink), respectively. The drain voltage was −200 V. (c,d) Optical micrographs of light emissions from a tetracene FET and a DCM1-doped tetracene crystal FET, respectively, from the top view.

ciency.[28−31] 4-(Dicyanomethylene)-2-methyl-6-(*p*-dimethylaminostyryl)-4*H*-pyran (DCM1),[32] whose highest occupied molecular orbital−lowest unoccupied molecular orbital (HOMO−LUMO) gap is smaller than that of tetracene (Figure 1d), was employed as the dopant.

DISCUSSION

Pristine and DCM1-Doped Tetracene Crystal. Crystals of pristine and DCM1-doped tetracene were prepared by physical vapor transport, and they were verified to be single crystals by a polarization microscope, a scanning electron microscope, an atomic-force microscope, and an X-ray diffractometer (refer to Supporting Information). Figure 2a displays the photoluminescence (PL) spectra of pure tetracene crystals (green curve), dichloromethane solution of DCM1 (gray curve), and DCM1-doped tetracene crystals (pink curve). The pristine tetracene crystals exhibited their PL spectra with peaks at 539, 574, 615, and 673 nm, while the dichloromethane solution of DCM1 shows a broad emission at 613 nm. As for the DCM1-doped crystals, the peak positions of the spectrum are similar to those of the pure tetracene crystals. However, the relative intensity from 580 to 700 nm, where DCM1 shows emission, is higher than that in the pure tetracene crystals. This phenomenon illustrates that both the tetracene and DCM1 emit light in the doped crystals.

External quantum efficiencies (EQEs) of the pure and doped crystals were 1 and 8%, respectively. Although the EQE of the doped crystal is not remarkably high, it is sufficient for demonstrating the new device concept. The quantum yield for singlet fission in the tetracene crystal was previously estimated to be 200%,[33] because its lifetime (80 ps) is much shorter than other competing processes, for example fluorescence decay (lifetime is 4.2 ns). Time-resolved PL of tetracene crystals at 540 nm showed prompt and delayed fluorescence (see Supporting Information). Delayed fluorescence in tetracene single crystals was already reported and was attributed to emission after singlet fission and succeeding triplet fusion.[33] DCM1-doped crystals also showed similar behavior at 540 nm in wavelength, indicating that the process can also occur in the crystals. In addition, DCM1-doped crystals showed prompt and delayed fluorescence at 650 nm in wavelength. Because the emission at the wavelength mostly comes from DCM1 molecules in the crystal, the delayed fluorescence indicates exciton can be transferred from tetracene to DCM1 after singlet fission and triplet fusion process as illustrated in Figure 1c.

L_{ex} in a tetracene crystal was evaluated by the method described in ref 12 (see Supporting Information for details). The obtained L_{ex} along the thickness direction was 1.87 μm, which is longer than the thicknesses of tetracene crystals employed in this study (several hundred nanometers). This micrometer-scale result corresponds well to the reports on singlet fission in tetracene crystals,[34,35] which generate triplet excitons with long L_{ex}.

Transport properties of both pristine and DCM1-doped tetracene crystals were characterized by FET measurements. For enhancing carrier injection and transport, asymmetric top-contact electrodes (Au−Ca) were used, and a SiO_2 dielectric layer was coated with poly(methyl methacrylate) (PMMA). Figure 2b shows transfer characteristics of the FETs based on a pristine and doped tetracene crystal. The drain voltage (V_D) was −200 V and the gate voltage (V_G) was varied from 0 to −200 V. Although both showed an ambipolar behavior, a drain current in DCM1-doped tetracene FET was 1 order lower than that of the pristine tetracene FET. Furthermore, saturated

DOI: 10.1021/acsami.9b02298
ACS Appl. Mater. Interfaces 2019, 11, 20200−20204

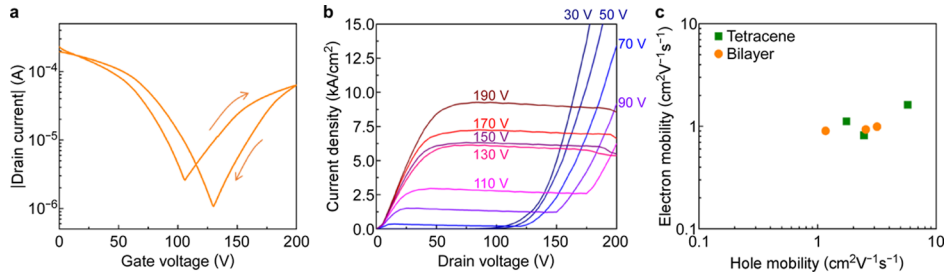

Figure 3. Performances of bilayer FETs. (a) Transfer characteristics at V_D = 200 V. (b) Output characteristics. (c) Hole and electron mobilities of bilayer FETs (orange filled circles) and those of tetracene FETs (green filled squares).

carrier mobilities of hole (μ_h) and electron (μ_e) were 0.33 and 1.28 cm^2 V^{-1} s^{-1}, respectively, in the pristine tetracene crystal FET. On the other hand, μ_h = 0.12 cm^2 V^{-1} s^{-1} and μ_e = 0.13 cm^2 V^{-1} s^{-1} in the DCM1-doped crystal FET, which indicates that DCM1 dopant molecules create electron traps as imagined from the deep LUMO of DCM1 compared with that of tetracene shown in Figure 1d. Because of the ambipolar behaviors, electroluminescence was observed in both FETs. Corresponding to their PL emission colors, pristine tetracene and DCM1-doped tetracene FETs showed green (Figure 2c) and red (Figure 2c) emissions, respectively.

Bilayer Light-Emitting Transistor. All the above experimental results indicate that pristine tetracene and DCM1-doped tetracene crystals are suitable as a transport layer (bottom layer) and a light-emitting layer (top layer), respectively, in a bilayer LE-OFET (Figure 1b). In the device, a CsF layer was inserted between a tetracene crystal and a Ca electrode to decrease the electron-injection resistance.[10] Figure 3a–c are device performances of a bilayer FET. From the transfer characteristics at V_D = 200 V (Figure 3a), mobilities, μ_h = 3.17 cm^2 V^{-1} s^{-1} and μ_e = 0.99 cm^2 V^{-1} s^{-1} for forward sweep and μ_h = 2.23 cm^2 V^{-1} s^{-1} and μ_e = 1.90 cm^2 V^{-1} s^{-1} for backward sweep, were obtained. Such high mobilities ensure the high current density.

Figure 3b shows output characteristics of the same FET, where an ambipolar behavior is observed in the V_G range from 70 to 110 V. The highest ambipolar current density reached the value as high as 11.2 kA/cm^2 (assuming that the accumulation layer thickness is equal to one molecular layer thickness of 1.2 nm, which was measured with an atomic force microscope). This high current density is comparable to 10.3 kA/cm^2, which is the threshold of lasing for a highly luminescent 5,5″-bis(biphenyl-4-yl)-2,2′:5′,2″-terthiophene single crystal FET estimated by Bisri et al.[9] Figure 3c shows the mobilities of bilayer FETs as well as single layer tetracene FETs, being fabricated and measured in the same condition. No clear separation between single-layer and bilayer FETs was observed from this result, indicating that the existence of the top layer would not affect the carrier transportation in the bottom layer.

Figure 4b shows a bird's-eye view optical micrograph of light emission from the bilayer FET illustrated in Figure 4a. The light-emission colors observed in the two layers were drastically different, that is, the bottom layer (pristine tetracene) displays a green color, while the top layer (DCM1-doped tetracene) displays a red color. The spectra of emissions from a single-layer part and a bilayer part in a bilayer FET were observed by microscopic spectroscopy and are shown in Supporting Information. The spectra elucidate that the color difference is due to the relatively large intensity

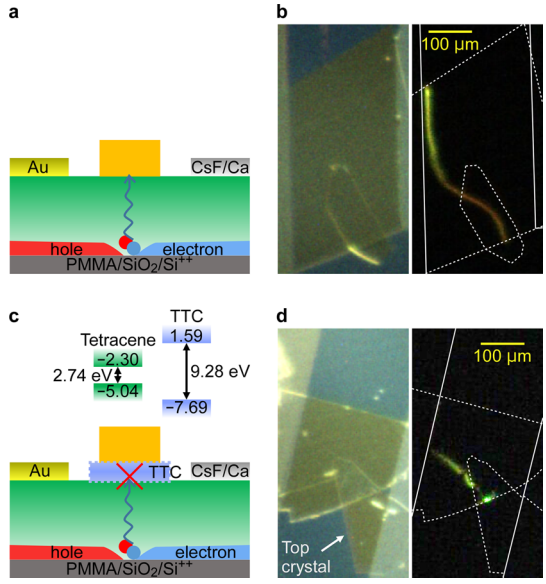

Figure 4. Light emission from bilayer FETs. (a) Schematic diagram of a bilayer FET. (b) Top-view optical micrograph of the bilayer transistor in the light (left) and its light emission in the dark (right). (c) Schematic construction of a TTC-inserted bilayer FET, and energy diagrams of TTC and tetracene; (d) Top-view optical micrograph of light emission from the TTC-inserted bilayer transistor in the light (left) and its light emission in the dark (right).

at the wavelength longer than 600 nm in the spectrum of the bilayer part. The results indicate that although the molecules in the bottom layer were excited by carrier recombination, a substantial part of the energy was transferred to the top layer. The top layer can be excited by two different mechanisms: the exciton diffusion from the bottom layer or the absorption of the light-emission from the bottom layer.

To confirm the excitation mechanism, a tetratetracontane ($CH_3(CH_2)_{42}CH_3$, TTC) layer of 6 nm in thickness was deposited between the pristine and DCM1-doped tetracene crystals (refer to Figure 4c). TTC is a transparent insulator with a HOMO–LUMO gap of 9.28 eV, and thus it blocks the exciton diffusion from one crystal to another but allows the transmission of light. The absorption spectrum of a TTC thin film of 30 nm in thickness on a quartz substrate was measured, and the transmittance of a TTC thin film of 6 nm in thickness is calculated to be >99.8% in the wavelength region of 400–900 nm. Figure 4d shows a bird's-eye view optical micrograph of the light emission from a TTC-inserted bilayer LE-OFETs. There was no difference in the emission color between the single-layer part and the bilayer part, which indicates that the top crystal was not excited. Thus, it is concluded that the top

DOI: 10.1021/acsami.9b02298
ACS Appl. Mater. Interfaces 2019, 11, 20200–20204

crystal was excited by the exciton diffusion from the bottom crystal. Exciton transfer from the bottom crystal to the top crystal requires good contact between the crystals. Scanning electron microscopy revealed that they have smooth surfaces and a good contact as shown in Supporting Information.

Mechanistical Discussion. The above results support the following mechanism of the light emission in the bilayer FETs. The excitons are generated by a carrier recombination process in the bottom of the bottom tetracene crystal. The quantum efficiency of the singlet and triplet generations in this process is 0.25 and 0.75, respectively. The generated singlets are immediately converted into triplets, and the formed triplets are 1.25 (=0.75 + 2 × 0.25) in quantum yield. Then, the triplets diffuse through a crystal and reach the bilayer interface with the probability of $\exp(-d/L_{ex})$, where d is the thickness of the bottom crystal and L_{ex} is the triplet exciton diffusion length of the bottom crystal along the c axis, as described above. The possibility of the triplets migrating to the bilayer interface is 0.732, when the thickness (583 nm) of the bottom crystal in a specific transistor is used. Therefore, the quantum yield of triplets, which reaches the interface, is 0.915 (=1.25 × 0.732). Although not all excitons pass through the interface, it is expected that a substantial number of excitons are transferred from the FET channel to the top crystal. The transferred triplet excitons are converted into singlet excitons by triplet fusion in the top crystal and emit light.

CONCLUSIONS

In conclusion, bilayer LE-OFETs composed of a tetracene crystal carrier transporter (bottom layer) and a DCM1-doped tetracene crystal light emitter (top layer) were fabricated. Red light emission, which is distinct from the green light emission of tetracene, was observed in the top crystal. When a TTC thin film was inserted between the bottom and top crystals, the top crystal did not emit light, indicating that excitons were blocked by the TTC thin films. These results confirmed that excitons formed in the bottom crystal diffuse to the top crystal and emit light. The separation of the carrier-transport and light-emission functions in the bilayer LE-OFETs will open a way for achieving the high carrier mobility and high luminescent efficiency required for high-performance LE-OFETs and electrically driven organic lasers.

MATERIALS AND METHODS

Preparation of Samples. Tetracene (99.9%) and DCM1 (98%) were purchased from Sigma-Aldrich. Both the pure and doped tetracene crystals were grown by physical vapor transport in a stream of argon gas (99.9999%). A mixture of tetracene 90 wt% and DCM1 10 wt% was used as the source material for the growth of doped crystals. The crystalline phase was characterized by a polarizing optical microscope, a scanning electron microscope, an atomic-force microscope, and an X-ray diffractometer.

Optical Properties. PL spectra were measured with a PL spectrophotometer (HITACHI: F-7000) with an excitation wavelength of 480 nm. EQEs were measured under excitation at 530 nm with a photocounting method using an integrating sphere and a Hamamatsu Photonics C9920-02 spectrometer.

FET Device Fabrication. A heavily p-type doped silicon wafer with a 300 nm thick SiO_2 film was used as a gate electrode and a gate dielectric layer. To reduce the electron traps at the interface between the gate dielectric layer and organic semiconductor, a 30 nm thick PMMA film was spin-coated from a toluene solution onto the SiO_2 surface. The whole gate substrate was heated overnight in the argon atmosphere at 75 °C. A single crystal was electrostatically attached to the prepared substrate. Au (100 nm) and CsF (1 nm)/Ca (500 nm), for the hole and electron injecting electrodes, were deposited on the single crystal by vacuum evaporation with the shadow mask technique. For bilayer LE-OFETs fabrications, a DCM1-doped crystal was laminated on the center position of the tetracene crystal before the electrode depositions. There was no contact between the top crystal and electrodes.

TTC Deposition and Transmittance Measurement. A TTC thin film with a thickness of 6 nm was deposited on the center position of the tetracene crystal, and then a DCM1-doped tetracene crystal was laminated on the TTC thin film. The following procedures were the same as in fabricating a regular bilayer FET.

A TTC thin film with a thickness of 30 nm was deposited on a quartz substrate, and its absorption spectrum was measured with a JASCO Corp. V-750 UV−visible spectrophotometer.

Exciton Diffusion Length. The thicknesses of the crystals were measured by a Veeco Dektak 150 surface profiler, which scanned over the whole length of a crystal placed on a quartz substrate. The angular dependence of the absorption coefficient was measured by recording an optical transmission through a very thin (867 nm) platelet-like tetracene single crystal with a UV−vis spectrophotometer (JASCO: V-650DS). The photocurrent measurements were carried out on the largest natural facet of the crystals, that is, the ab facet, in a coplanar contact configuration. Electrical contacts were prepared with silver paste, and the photocurrent was measured by a Keithley K2400 source meter. The crystal surface was illuminated at a normal incidence using monochromatic light with a wavelength of 405 nm obtained with a continuous laser. A liner polarizer was used to produce polarized light.

Theoretical Calculations. All molecular orbitals were calculated with the Gaussian 03 package using the B3LYP/cc-pVDZ method, which is a hybrid method combining the density-functional theory and the Hartree−Fock method.

ASSOCIATED CONTENT

Supporting Information

The Supporting Information is available free of charge on the ACS Publications website at DOI: 10.1021/acsami.9b02298.

> Crystal growth and characterization; time-resolved PL; measurement of exciton diffusion length; field-effect mobilities of monolayer FETs; microscopic spectroscopy of emission; and contact between two crystals (PDF)

AUTHOR INFORMATION

Corresponding Authors

*E-mail: shimotani@tohoku.ac.jp (Hidekazu Shimotani).
*E-mail: tanigaki@m.tohoku.ac.jp (K.T.).

ORCID

Hidekazu Shimotani: 0000-0003-3238-9420

Present Addresses

⊥T.K.: Department of Physics, Indian Institute of Science Education and Research (IISER), Tirupati 517507, India
§Institute of Condensed Matter and Nanosciences (IMCN/NAPS), Université catholique de Louvain, 1348 Louvain-la-Neuve, Belgium.

Author Contributions

H. Shang and H. Shimotani conceived the experiments. H. Shimotani and K.T. supervised the project. H. Shang carried out almost all the experiments and wrote the manuscript. H. Shimotani performed theoretical calculation. T.K. provided technique of CsF and TTC thin-film deposition.

Funding

This work was supported by JSPS KAKENHI grant numbers 24684023 and 25610084. H. Shang is grateful for the CSC

DOI: 10.1021/acsami.9b02298
ACS Appl. Mater. Interfaces 2019, 11, 20200−20204

scholarship from Chinese government as well as the Tohoku University President Scholarship for Research and Education.

Notes

The authors declare no competing financial interest.

REFERENCES

(1) Pisignano, D.; Anni, M.; Gigli, G.; Cingolani, R.; Zavelani-Rossi, M.; Lanzani, G.; Barbarella, G.; Favaretto, L. Amplified Spontaneous Emission and Efficient Tunable laser Emission from a Substituted Thiophene-Based Oligomer. *Appl. Phys. Lett.* **2002**, *81*, 3534−3536.
(2) Samuel, I. D. W.; Namdas, E. B.; Turnbull, G. A. How to Recognize Lasing. *Nat. Photonics* **2009**, *3*, 546−549.
(3) Fang, H.-H.; Ding, R.; Lu, S.-Y.; Yang, J.; Zhang, X.-L.; Yang, R.; Feng, J.; Chen, Q.-D.; Song, J.-F.; Sun, H.-B. Distributed Feedback Lasers Based on Thiophene/Phenylene Co-Oligomer Single Crystals. *Adv. Funct. Mater.* **2012**, *22*, 33−38.
(4) Hide, F.; Diaz-Garcia, M. A.; Schwartz, B. J.; Andersson, M. R.; Pei, Q.; Heeger, A. J. Semiconducting Polymers: A New Class of Solid-State Laser Materials. *Science* **1996**, *273*, 1833−1836.
(5) Tessler, N.; Denton, G. J.; Friend, R. H. Lasing from conjugated-polymer microcavities. *Nature* **1996**, *382*, 695−697.
(6) Li, X.; Gao, N.; Xu, Y.; Li, F.; Ma, Y. Self-Cavity Laser Oscillations with Very Low Threshold from a Symmetric Organic Crystal Waveguide. *Appl. Phys. Lett.* **2012**, *101*, 063301.
(7) Gwinner, M. C.; Khodabakhsh, S.; Song, M. H.; Schweizer, H.; Giessen, H.; Sirringhaus, H. Integration of a Rib WaveGuide Distributed Feedback Structure into a Light-Emitting Polymer Field-Effect Transistor. *Adv. Funct. Mater.* **2009**, *19*, 1360−1370.
(8) Yamao, T.; Sakurai, Y.; Terasaki, K.; Shimizu, Y.; Jinnai, H.; Hotta, S. Current-Injected Spectrally-Narrowed Emissions from an Organic Transistor. *Adv. Mater.* **2010**, *22*, 3708−3712.
(9) Bisri, S. Z.; Takenobu, T.; Yomogida, Y.; Shimotani, H.; Yamao, T.; Hotta, S.; Iwasa, Y. High Mobility and Luminescent Efficiency in Organic Single-Crystal Light-Emitting Transistors. *Adv. Funct. Mater.* **2009**, *19*, 1728−1735.
(10) Sawabe, K.; Imakawa, M.; Nakano, M.; Yamao, T.; Hotta, S.; Iwasa, Y.; Takenobu, T. Current-Confinement Structure and Extremely High Current Density in Organic Light-Emitting Transistors. *Adv. Mater.* **2012**, *24*, 6141−6146.
(11) Maruyama, K.; Sawabe, K.; Sakanoue, T.; Li, J.; Takahashi, W.; Hotta, S.; Iwasa, Y.; Takenobu, T. Ambipolar Light-Emitting Organic Single-Crystal Transistors with a Grating Resonator. *Sci. Rep.* **2015**, *5*, 10221.
(12) Cornil, J.; dos Santos, D. A.; Crispin, X.; Silbey, R.; Brédas, J. L. Influence of Interchain Interactions on the Absorption and Luminescence of Conjugated Oligomers and Polymers: A Quantum-chemical Characterization. *J. Am. Chem. Soc.* **1998**, *120*, 1289−1299.
(13) Cornil, J.; Beljonne, D.; Calbert, J.-P.; Brédas, J.-L. Interchain Interactions in Organic π-Conjugated Materials: Impact on Electronic Structure, Optical Response, and Charge Transport. *Adv. Mater.* **2001**, *13*, 1053−1067.
(14) Shuai, Z.; Geng, H.; Xu, W.; Liao, Y.; André, J.-M. From Charge Transport Parameters to Charge Mobility in Organic Semiconductors Through Multiscale Simulation. *Chem. Soc. Rev.* **2014**, *43*, 2662−2679.
(15) Mutai, T.; Satou, H.; Araki, K. Reproducible on-off switching of solid-state luminescence by controlling molecular packing through heat-mode interconversion. *Nat. Mater.* **2005**, *4*, 685.
(16) Xie, Z.; Yang, B.; Li, F.; Cheng, G.; Liu, L.; Yang, G.; Xu, H.; Ye, L.; Hanif, M.; Liu, S.; Ma, D.; Ma, Y. Cross Dipole Stacking in the Crystal of Distyrylbenzene Derivative: The Approach toward High Solid-State Luminescence Efficiency. *J. Am. Chem. Soc.* **2005**, *127*, 14152−14153.
(17) Swenberg, C.; Pope, M. *Electronic Processes in Organic Crystals and Polymers*, 2th ed.; Oxford University Press, 1999.
(18) Lunt, R. R.; Giebink, N. C.; Belak, A. A.; Benziger, J. B.; Forrest, S. R. Exciton Diffusion Lengths of Organic Semiconductor Thin Films Measured by Spectrally Resolved Photoluminescence Quenching. *J. Appl. Phys.* **2009**, *105*, 053711.
(19) Yang, L.-G.; Chen, H.-Z.; Wang, M. Optimal Film Thickness for Exciton Diffusion Length Measurement by Photocurrent Response in Organic Heterostructures. *Thin Solid Films* **2008**, *516*, 7701−7707.
(20) Najafov, H.; Lee, B.; Zhou, Q.; Feldman, L. C.; Podzorov, V. Observation of Long-range Exciton Diffusion in Highly Ordered Organic Semiconductors. *Nat. Mater.* **2010**, *9*, 938−943.
(21) Akselrod, G. M.; Deotare, P. B.; Thompson, N. J.; Lee, J.; Tisdale, W. A.; Baldo, M. A.; Menon, V. M.; Bulovic, V. Visualization of Exciton Transport in Ordered and Disordered Molecular Solids. *Nat. Commun.* **2014**, *5*, 3646.
(22) Irkhin, P.; Biaggio, I. Direct Imaging of Anisotropic Exciton Diffusion and Triplet Diffusion Length in Rubrene Single Crystals. *Phys. Rev. Lett.* **2011**, *107*, 017402.
(23) Zimmerman, P. M.; Bell, F.; Casanova, D.; Head-Gordon, M. Mechanism for Singlet Fission in Pentacene and Tetracene: from Single Exciton to Two Triplets. *J. Am. Chem. Soc.* **2011**, *133*, 19944−19952.
(24) Smith, M. B.; Michl, J. Singlet Fission. *Chem. Rev.* **2010**, *110*, 6891−6936.
(25) Ern, V.; Avakian, P.; Merrifield, R. E. Diffusion of Triplet Excitons in Anthracene Crystals. *Phys. Rev.* **1966**, *148*, 862−867.
(26) Takenobu, T.; Bisri, S. Z.; Takahashi, T.; Yahiro, M.; Adachi, C.; Iwasa, Y. High Current Density in Light-Emitting Transistors of Organic Single Crystals. *Phys. Rev. Lett.* **2008**, *100*, 066601.
(27) Burdett, J. J.; Müller, A. M.; Gosztola, D.; Bardeen, C. J. Excited State Dynamics in Solid and Monomeric Tetracene: The Roles of Superradiance and Exciton Fission. *J. Chem. Phys.* **2010**, *133*, 144506.
(28) Wang, H.; Li, F.; Gao, B.; Xie, Z.; Liu, S.; Wang, C.; Hu, D.; Shen, F.; Xu, Y.; Shang, H.; Chen, Q.; Ma, Y.; Sun, H. Doped Organic Crystals with High Efficiency, Color-Tunable Emission toward Laser Application. *Cryst. Growth Des.* **2009**, *9*, 4945−4950.
(29) Nakanotani, H.; Adachi, C. Amplified Spontaneous Emission and Electroluminescence from Thiophene/Phenylene Co-Oligomer-Dopedp-bis(p-Styrylstyryl)Benzene Crystals. *Adv. Opt. Mater.* **2013**, *1*, 422−427.
(30) Wang, H.; Zhao, Y.; Xie, Z.; Shang, H.; Wang, H.; Li, F.; Ma, Y. Preparation, Optical Property and Field-Effect Mobility Investigation of Stable White-Emissive Doped Organic Crystal. *CrystEngComm.* **2015**, *17*, 2168−2175.
(31) Shang, H.; Wang, H.; Gao, N.; Shen, F.; Li, X.; Ma, Y. Large organic single crystal sheets grown from the gas-liquid and gas-liquid-solid interface. *CrystEngComm* **2012**, *14*, 869−874.
(32) Capelli, R.; Toffanin, S.; Generali, G.; Usta, H.; Facchetti, A.; Muccini, M. Organic Light-Emitting Transistors with an Efficiency that Outperforms The Equivalent Light-Emitting Diodes. *Nat. Mater.* **2010**, *9*, 496−503.
(33) Thorsmølle, V. K.; Averitt, R. D.; Demsar, J.; Smith, D. L.; Tretiak, S.; Martin, R. L.; Chi, X.; Crone, B. K.; Ramirez, A. P.; Taylor, A. J. Morphology Effectively Controls Singlet-Triplet Exciton Relaxation and Charge Transport in Organic Semiconductors. *Phys. Rev. Lett.* **2009**, *102*, 017401.
(34) Akselrod, G. M.; Deotare, P. B.; Thompson, N. J.; Lee, J.; Tisdale, W. A.; Baldo, M. A.; Menon, V. M.; Bulovic, V. Visualization of Exciton Transport in Ordered and Disordered Molecular Solids. *Nat. Commun.* **2014**, *5*, 3646.
(35) Wan, Y.; Guo, Z.; Zhu, T.; Yan, S.; Johnson, J.; Huang, L. Cooperative Singlet and Triplet Exciton Transport in Tetracene Crystals Visualized by Ultrafast Microscopy. *Nat. Chem.* **2015**, *7*, 785−792.

DOI: 10.1021/acsami.9b02298
ACS Appl. Mater. Interfaces 2019, 11, 20200−20204